ChemComm

COMMUNICATION

View Article Online
View Journal

Cite this: DOI: 10.1039/d4cc05628k

Received 23rd October 2024,
Accepted 11th December 2024

DOI: 10.1039/d4cc05628k

rsc.li/chemcomm

Isolation of mixed valence charge-neutral Ag_{12}, and dicationic Ag_{10} nano-clusters stabilized by carbene-phosphaalkenides†

Maria Francis, ‡[a] Asutosh Patra, ‡[a] Farsana Abdul Salam, [a] Siriyara Jagannatha Prathapa[b] and Sudipta Roy *[a]

Cyclic alkyl(amino) carbene (cAAC)-supported phosphaalkenides (cAAC═P)$^-$ have been employed as ligands for the isolation of two atomically precise mixed valence paramagnetic $Ag^{I/0}_{12}Cl_3$, and $Ag^{I/0}_{10}$, nano-clusters [$(Me_2$-cAAC═P$)_6Ag_{12}Cl_3$] (2), and [$(Me_2$-cAAC═P$)_6Ag_{10}](NTf_2)_2$ (4). 2 and 4 have been structurally characterized by single-crystal X-ray diffraction revealing the presence of three Ag^0 atoms, nine Ag^I ions (2); and two Ag^0 atoms, eight Ag^I ions (4), respectively. The clustering inorganic unit $Ag_{12}Cl_3$ in 2 has been found to be surrounded by six mono-anionic μ_3-cAAC═P moieties having 3-bar symmetry. 2 and 4 have been studied by cyclic voltammetry, UV-vis, ESI-MS, XPS, EPR spectroscopy, and DFT calculations.

Silver nanoclusters (NCs) are known to exhibit unique electronic, and optical properties, such as strong photoluminescence, and various catalytic activities.[1] They are utilised as attractive luminescent probes for sensing and bioimaging.[2] Structurally well-defined NCs possessing Ag^0 atoms are highly reactive, and easier to oxidize compared to their heavier Au analogues, which makes their synthesis challenging. Metallic silver is non-magnetic in its bulk form. However, Pereiro *et al.* theoretically predicted that the small nuclearity silver NCs, Ag_n, could be magnetic with variation of the magnetic moment depending on the value of n [n = 2–22].[3] Liu *et al.* reported the isolation of the chiral open-shell Ag_{23} NC with five Ag^0 atoms, which was structurally characterized by single-crystal X-ray diffraction.[4] The open-shell behaviour of this Ag_{23} NC was confirmed by a weak electron paramagnetic resonance (EPR) signal, characteristic of s = 1/2, with g = 1.959 and 1.955.[4] The first atomically precise mixed valence $Ag^{0/I}_{22}$ NC displaying thermally activated delayed fluorescence (TADF) was reported in 2022 by Sun and co-workers.[5] In the same year, two other mixed valence NCs $Ag^{0/I}_8$ and $Ag^{0/I}_{29}$ exhibiting strong EPR signals were reported.[6] The heavily Ag^0-doped KCl:AgCl crystals in different chemical defect positions [cationic and anionic holes] were studied by EPR spectroscopy.[7a] The generation of Ag_4^{3+}, and Ag_6^+ clusters was also reported under different chemical conditions.[7b,c] However, the mixed valence silver NCs are rarely reported.[8] The first closed-shell mixed valence $Ag_2^{I/III}$ [Ag···Ag 7.4 Å] containing N_8-donor macrocyclic ligand was isolated by Qin-Hui *et al.* in 1994.[9a] The 1D zig-zag chain of $Ag_2^{I/II}$ (ref. 9*b*) stabilized by the cyclic alkyl(amino) carbene (cAAC)-supported mono-anion of the inversely polarized phosphaalkene, *viz.*, the phosphaalkenide[10] was reported by Roy and co-workers. N-heterocyclic carbene (NHC), and P-$SiMe_3$ ligated diamagnetic Ag^I_{12}, and Ag^I_{26} clusters were reported by Corrigan *et al.*[11] A plethora of other Ag^I clusters have been synthesized, and characterized employing alkyne, thiolate, sulfide, selenide, phosphine, perchlorate, *etc.* as ligands.[12] Moreover, clusters with Ag–H moieties have also been isolated, and further studied by mass spectrometry.[13] However, isolation of stable silver NCs introducing carbene-phosphaalkenides as ligands is still scarce. Herein, we report on the solid-state isolation, and structural characterization of two novel structurally well-defined mixed valence paramagnetic silver NCs with $Ag^{I/0}_{12}Cl_3$, and $Ag^{I/0}_{10}$ metallic cores.

The dark red crystals of Me_2-cAAC═P–K (**1**)[14] (Me_2-cAAC═C(*N*-2,6-$^i Pr_2C_6H_3$)$(CMe_2)_2(CH_2)$) were reacted with $AgNTf_2$ in a 3 : 2 molar ratio in toluene at 0 °C to room temperature (rt) for 12 h to obtain a dark brown-red reaction mixture. Upon drying, the resultant crystalline solid obtained was dissolved in freshly distilled DCM, and stored for crystallization upon concentration to ∼1 mL in a freezer at −40 °C. After one-week, dark red blocks of [$(Me_2$-cAAC═P$)_6(Ag)_{12}(Cl)_3$] (**2**) were isolated in 40% yield (Scheme 1). The presence of the three chloride ions in **2** can be attributed to the decomposition of DCM, the usage of which is found to be crucial for the isolation of **2**. A different mixed valence dicationic cluster [$(Me_2$-cAAC═P$)_6(Ag)_{10}](NTf_2)_2$ (**4**) was isolated in 60% yield as yellow blocks when [Me_2-cAAC═P–B(N(^{i}Pr)$_2)_2$] (**3**)[9b] was reacted with $AgNTf_2$ in 2 : 1

[a] Department of Chemistry, Indian Institute of Science Education and Research (IISER) Tirupati, Tirupati 517619, India. E-mail: roy.sudipta@iisertirupati.ac.in
[b] Bruker India Scientific Pvt. Ltd, India

† Electronic supplementary information (ESI) available. CCDC 2242239 (**2**), 2194453 (**4**). For ESI and crystallographic data in CIF or other electronic format see DOI: https://doi.org/10.1039/d4cc05628k

‡ Both authors contributed equally.

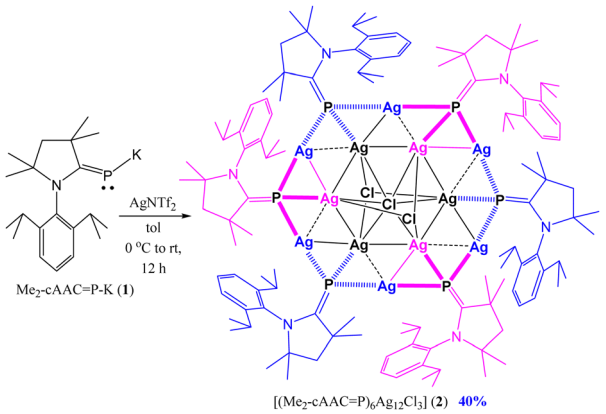

Scheme 1 Synthesis of mixed-valence neutral NC [(Me$_2$-cAAC═P)$_6$Ag$_{12}$(Cl$_3$)] (**2**).

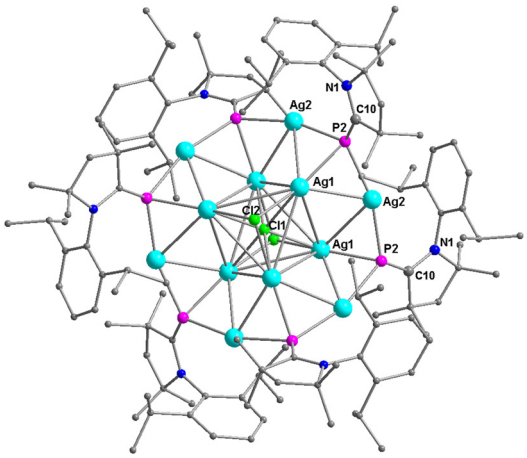

Fig. 1 Molecular structure of NC [(Me$_2$-cAAC═P)$_6$(Ag)$_{12}$(Cl$_3$)] (**2**). Hydrogen atoms are omitted for clarity.

molar ratio in toluene at rt for 12 h, followed by crystallization of the resultant precipitate from concentrated DCM solution, stored at 0 °C in a refrigerator (Scheme 2). The (cAAC═P)$^-$ ligands are found to be redox non-innocent, and undergo oxidation to produce the corresponding radical followed by dimerization, resulting in the formation of (Me$_2$-cAAC)$_2$P$_2$ with a subsequent reduction of Ag^I to Ag^0 in solution affording the mixed valence Ag-NCs **2** and **4**.[6] The presence of Ag^0 and Ag^I centres in **2** and **4** is supported by XPS spectroscopy (see ESI†). The formation of (Me$_2$-cAAC)$_2$P$_2$ in the reaction mixture is confirmed by ^{31}P NMR spectroscopy (δ = 55.1 ppm).

The red/yellow blocks of **2**/**4** are found to be stable under an argon atmosphere for six months inside a glove box at rt. The powders of **2** and **4** decompose above 205 and 165 °C, respectively. **2** and **4** are found to be NMR silent, and EPR active.

2 and **4** have been structurally characterized by single-crystal X-ray diffraction. The dodeca-nuclear Ag-NC [(Me$_2$-cAAC═P)$_6$-(Ag)$_{12}$(Cl)$_3$] (**2**) crystallizes in the trigonal $R\bar{3}$ space group (Fig. 1). **2** comprises six (Me$_2$-cAAC═P)$^-$ ligands, three chloride ions, and twelve Ag-atoms/ions. Fig. 2 shows that the asymmetric unit of **2** starting at position-1, generates six different symmetry equiv. points (1–6). Positions 1, 3 and 5 are non-inverted, while positions 2, 4 and 6 are three inverted-symmetry equiv. positions. There are three Ag^0 atoms in **2**, which is

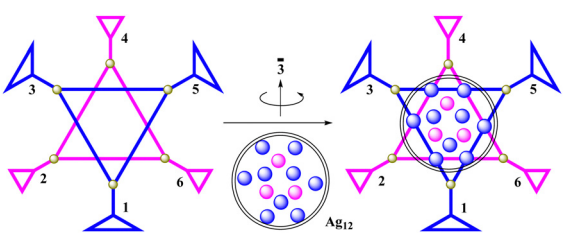

Fig. 2 Structural topology and symmetry [3-bar] in NC **2**.

suggested from charge balance consideration, since there are a total of nine mono-anionic ligands present.

The space filling model of **2** has been shown in Fig. 3 (left), which represents how the central Ag$_{12}$ metallic core is well protected by the surrounding cAAC-supported phosphaalkenide ligands. The natural bond orbital (NBO) analyses of NCs **2** and **4** at neutral doublet, and dicationic triplet states, respectively, were performed at the UBP86-D3(BJ)/Def2-SVP level of theory (see ESI† for details). The NBO analysis of **2** revealed that the α-LUMO+1, α-LUMO, and α-SOMO are very close in energy (ΔE = 0.01–0.05 eV) suggesting that the unpaired electron in **2** can span all these three orbitals involving the C═N–P unit, Cl and Ag atoms (see ESI†). This is also reflected in the Mulliken α-spin densities of **2** showing delocalization of spin densities due to the unpaired electron (Fig. 3 (right), see ESI†).

The Ag–Ag distances of charge-neutral NC **2** are found to be 2.883(1), and 3.024(2) Å, which are significantly shorter than

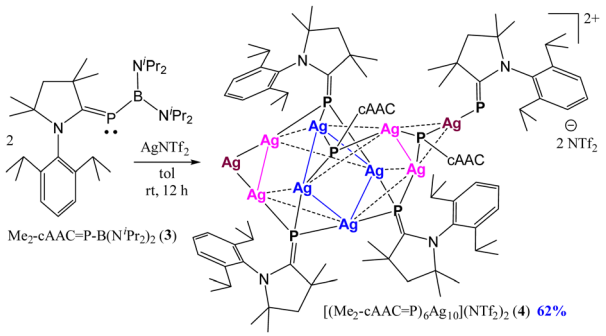

Scheme 2 Synthesis of mixed-valence dicationic NC [(Me$_2$-cAAC═P)$_6$Ag$_{10}$]-(NTf$_2$)$_2$ (**4**).

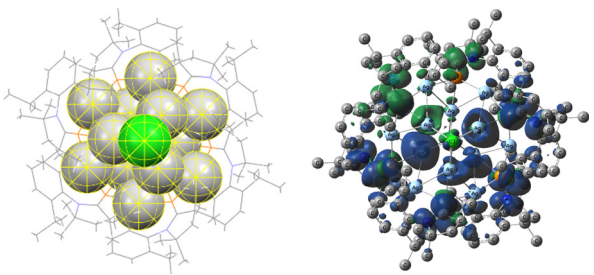

Fig. 3 Space filling model (left), and Mulliken α-spin densities (right) of [(Me$_2$-cAAC═P)$_6$Ag$_{12}$Cl$_3$] (**2**).

those of the previously isolated tri-cationic closed-shell Ag NC $\mathbf{2}^{3+}(OTf^-)_3$ (2.9593(14), 2.9174 (12), 3.2026(15), 3.1541(13) Å).[6] The Ag–P distances of **2** are 2.379(4), 2.401(3), and 2.455(2) Å, which are close to those of $\mathbf{2}^{3+}(OTf^-)_3$ (Ag–P 2.393(4)–2.431(4) Å).[6] The C–P bond in **2** is 1.75(1) Å, which is slightly shorter than those of $\mathbf{2}^{3+}(OTf^-)_3$ (1.780(11)–1.801(11) Å).[6] The Ag–Cl distances in **2** are found to be 2.4530(14), and 2.572(7) Å, which are either very similar in value or significantly smaller than those of $\mathbf{2}^{3+}$ (2.475(9), 2.705(5), 2.638 (4), 2.7143(11), 2.732(4), 2.8254(10) Å).[6] The diameter of the outer/peripheral Ag_6 ring of **2** having a three-fold symmetry is 8.37 Å, which is very close to those of $\mathbf{2}^{3+}$ with two-fold symmetry (8.26, 8.36, 8.48 Å).[6] The Cl–Cl distance between the two extreme Cl-ions in **2** is 5.8 Å, which is shorter than that of $\mathbf{2}^{3+}$ (6.5 Å).[6] The P–P distance in **2** is 9.02 Å, which is slightly greater than the average value of $\mathbf{2}^{3+}$ (8.46 Å; 8.26, 8.36, 4.48, 8.88, 9.22 Å).[6] **2** represents the first example of an $Ag^{I/0}$ based mixed valence NC, which has been structurally characterized in two different charged (0 (**2**) *vs.* +3 ($\mathbf{2}^{3+}$)], and spin states [doublet (**2**) *vs.* singlet ($\mathbf{2}^{3+}$)).[6]

The dicationic deca-nuclear Ag NC $[(Me_2\text{-cAAC}{=}P)_6Ag_{10}](NTf_2)_2$ (**4**) crystallizes in triclinic space group $P\bar{1}$ (Fig. 4). The entire molecule of **4** appears in the crystallographic asymmetric unit, which possesses six mono-anionic ligands $(Me_2\text{-cAAC}{=}P)^-$, and ten Ag-atoms/ions. There are two non-coordinating/free mono-anionic NTf_2^- anions present for the electrical charge balance. The charge balance consideration suggests that there are two Ag^0 atoms in **4**. The four arms of the central Ag_4 unit of **4** have been bridged by four P-atoms of mono-anionic Me_2-cAAC$=P^-$ ligands producing a $(Me_2\text{-cAAC}{=}P)_4Ag_4$ unit. Two Ag_2 units have been placed in anti-fashion above and below the irregular square-like Ag_4 unit (Fig. 4 and 5).

An additional Ag-atom is present above the Ag_2 unit (Fig. 4 and 5), while another Ag atom is bridged by a μ_3-P atom (right, Fig. 5). The Ag–Ag distances of the central four-membered Ag_4 ring in **4** are 2.90, 3.0, and 3.20 Å, which are longer than those (~2.96 Å) of the $Ag_8^{0/I}$ complex.[6]

The Ag_2 unit, which is situated on the top of the central Ag_4 unit, possesses the Ag–Ag distance of 2.91 Å, which is significantly shorter than that of the Ag_3 triangle of **4** (3.04 Å). The corresponding Ag–Ag distance in previously reported $Ag_8^{0/I}$ complexes is 3.07 Å.[6] Notably, the distal Ag atom (Ag9) (Ag7–Ag9, Ag8–Ag9; 2.472(3), 2.458(3) Å) is significantly closer to the Ag_2 arm (Ag8–Ag9), which is situated above the central Ag_4 unit of **4**. The Ag–P bond lengths of NC $Ag_{10}^{0/I}$ (**4**) range from 2.23 Å to 2.48 Å, and are significantly different than those of the neutral Ag_8 cluster (2.404(5)–2.417(4) Å).[6] The space filling diagram of a ten Ag atoms/ions unit of **4** has been shown in Fig. 6 (left). The Ag atom placed above the Ag_2 unit is situated in between the two aromatic rings of the Dipp ligands. The NBO, and Mulliken spin density analyses of **4** (Fig. 6 (right)) showed the major spin densities on the C=N–P unit with very small values on the Ag-atoms except for one Ag-atom (5.6%) and thus typical EPR features of Ag–P systems were not observed[6] in the experimental EPR spectrum of **4**.

The EPR spectra of **2** and **4** (in DCM) are shown in Fig. 7 and 8. The EPR simulation/fitting of **2** considering coupling of the unpaired electron with the nuclei of $^{107,109}Ag$, ^{31}P and $^{35,37}Cl$ atoms is quite satisfactory (Fig. 7). Three board lines near g = 2.0033 were observed for the previously reported $Ag_8^{0/I}$ cluster containing four Ag^0 atoms.[6,9b] However, the EPR spectrum of **2** shows three sets of multiple hyperfine lines, which have been simulated with EasySpin.

The coupling constants of one $^{107,109}Ag^0$, two ^{31}P and one $^{35,37}Cl$ nuclei are 9.43, 111.79/111.75, and 9.81 MHz, respectively, with a slight rhombic nature of g [g_x = 2.00766, g_y = 2.00885, g_z = 1.99959]. The EPR spectrum of **4** appears as unsymmetrical showing two resonances around $g \approx 2$ [g_x = 2.00165, g_y = 2.00006, g_z = 1.99703] (Fig. 8). The coupling constant of Ag^0 is 2.51 MHz, which is significantly smaller than that of **2** (9.43 MHz). The ESI-MS studies show that **2** (see ESI†) and **4** can fly as dications. The ESI-MS spectrum of $\mathbf{4}^{2+}$ corroborates the loss of two isopropyl groups with the intake of a sodium ion as $[(Me_2cAACP)_6Ag_{10} + Na\text{–}2C_3H_7\text{–}H]^{2+}$. The cyclic

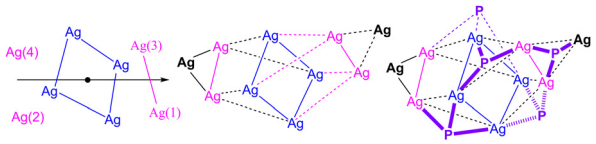

Fig. 5 Core topology of $[(Me_2\text{-cAAC}{=}P)_6Ag_{10}](NTf_2)_2$ (**4**). Two Ag_6 square prisms sharing the blue colored pseudo-Ag_4-square with a 4-bar symmetry operation.

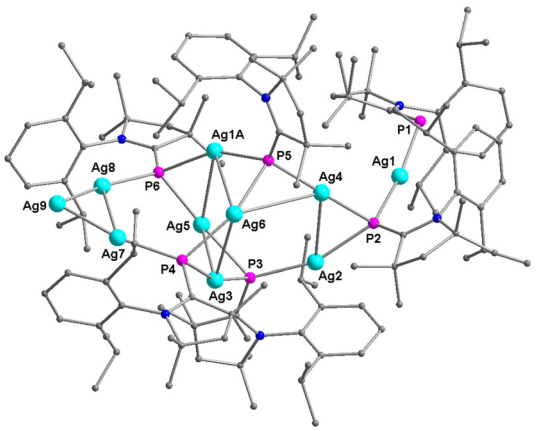

Fig. 4 Molecular structure of NC $[(Me_2\text{-cAAC}{=}P)_6Ag_{10}](NTf_2)_2$ (**4**). Hydrogen atoms are omitted for clarity. Two triflimide anions $[N(SO_2CF_3)_2^-]$ are omitted for clarity.

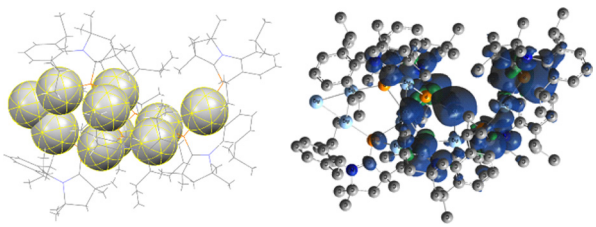

Fig. 6 Space filling model of total molecule (left), and Mulliken α-spin densities (right) of $[(Me_2\text{-cAAC}{=}P)_6Ag_{10}](NTf_2)_2$ (**4**).

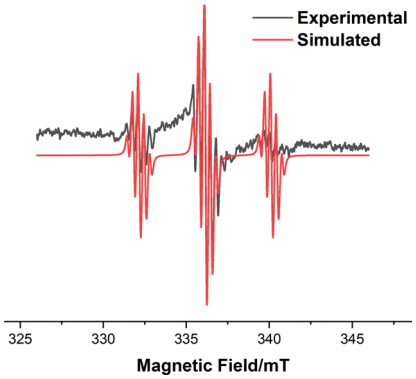

Fig. 7 Experimental (black), and simulated (red) X-band EPR spectra of $[(Me_2\text{-cAAC}{=}P)_6(Ag)_{12}(Cl_3)]$ (**2**) in DCM at 293 K. EasySpin, simulated parameters: one $^{107,109}Ag(0)$ [A = 9.43 MHz], two ^{31}P [A = 111.79, 111.75 MHz], one $^{35,37}Cl$ [A = 9.81 MHz], g_x = 2.00766, g_y = 2.00885, g_z = 1.99959, LW1 = 0.016 mT, LW2 = 0.166 mT. Experimental frequency = 9.436369 GHz.

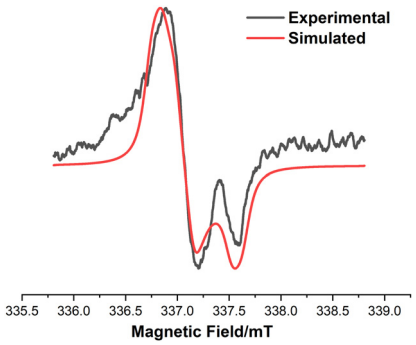

Fig. 8 X-band EPR spectrum of the NC $[(Me_2\text{-cAAC}{=}P)_6(Ag)_{10}](NTf_2)$ (**4**) in DCM at 293 K. Black line represents the experimental spectrum, and the red line represents the simulated spectrum using the EasySpin program [g_x = 2.00165, g_y = 2.00006, g_z = 1.99703, $LWPP_1$ = 0.0678384 mT, $LWPP_2$ = 0.0817786 mT, A_{Ag} = 2.51891 MHz].

voltammetry studies of **2** and **4** suggest the possible oxidation (see ESI†). The UV-vis spectra (in THF at 298 K) of **2** and **4** exhibited the absorption maxima (λ_{max}) at 365 and 367 nm, respectively (see ESI†). **2** and **4** were observed to be non-emissive.

In conclusion, two novel mixed valence Ag-NCs (Ag_{10}, **2**; Ag_{12}, **4**) were isolated as red/yellow blocks. **2** and **4** have been structurally characterized by X-ray single-crystal diffraction. The Ag_{10}, and Ag_{12} NCs possess three and two Ag^0 atoms, respectively. The NMR silent NCs **2** and **4** were found to be EPR active. The unpaired electrons couple with the $^{35,37}Cl$, ^{31}P and $^{107,109}Ag$ nuclei. The strongest coupling constant was obtained for ^{31}P-nuclei (111.75 MHz) in **2**. The coupling constant of $^{107,109}Ag$ of **2** (9.43 MHz) is four times stronger than that of **4** (2.51 MHz). The distributions of electron densities in **2** and **4** were estimated by computation of the Mulliken spin densities, and further correlated with ERP simulation.

SR gratefully acknowledges STARS-IISC, MoE (MoE-STARS/STARS-2/2023-0666), IISERT, CSIR for the generous financial support. We thank Dr S. S. Sen (NCL-Pune), and KB for the XPS measurements.

Data availability

The data supporting this article (experimental details, UV-vis, HRMS, EPR, XPS, single-crystal X-ray data, and computational details) have been included as part of the ESI.† Crystallographic data for **2** and **4** have been deposited at the CCDC (2242239, 2194453†), and can be obtained from **https://www.ccdc.cam.ac.uk/**.

Conflicts of interest

There are no conflicts to declare.

Notes and references

1 (*a*) C. M. Aikens, *J. Phys. Chem. Lett.*, 2011, **2**, 99; (*b*) Y. Du, H. Sheng, D. Astruc and M. Zhu, *Chem. Rev.*, 2020, **120**, 526.
2 (*a*) T. Udayabhaskararao and T. Pradeep, *J. Phys. Chem. Lett.*, 2013, **4**, 1553; (*b*) K. Zheng, X. Yuan, N. Goswami, Q. Zhang and J. Xie, *RSC Adv.*, 2014, **4**, 60581.
3 M. Pereiro, D. Baldomir and J. E. Arias, *Phys. Rev. A*, 2007, **75**, 063204.
4 C. Liu, T. Li, H. Abroshan, Z. Li, C. Zhang, H. J. Kim, G. Li and R. Jin, *Nat. Commun.*, 2018, **9**, 744.
5 Z.-R. Yuan, Z. Wang, B.-L. Han, C.-K. Zhang, S.-S. Zhang, Z.-Y. Zhu, J.-H. Yu, T.-D. Li, Y.-Z. Li, C.-H. Tung and D. Sun, *Angew. Chem., Int. Ed.*, 2022, **61**, e202211628.
6 E. Nag, S. Battuluri, K. C. Mondal and S. Roy, *Chem. – Eur. J.*, 2022, **28**, e202202324.
7 (*a*) P. G. Baranov, N. G. Romanov, V. A. Khramtsov and V. S. Vikhnin, *J. Phys.: Condens. Matter*, 2001, **13**, 2651; (*b*) J. Sadło, J. Michalik and L. Kevan, EPR and ESEEM study of silver clusters in ZK-4 molecular sieves, *Nukleonika*, 2006, **51**, 49; (*c*) A. Baldansuren, R. Eichel and E. Roduner, *Phys. Chem. Chem. Phys.*, 2009, **11**, 6664.
8 H. Hirai, S. Ito, S. Takano, K. Koyasu and T. Tsukuda, *Chem. Sci.*, 2020, **11**, 12233.
9 (*a*) Y. Shu-Yan, L. Qin-Hui and S. Meng-Chang, *Inorg. Chem.*, 1994, **33**, 1251; (*b*) E. Nag, S. Battuluri, B. B. Sinu and S. Roy, *Inorg. Chem.*, 2022, **61**, 3007.
10 L. Weber, U. Lassahn, H.-G. Stammler and B. Neumann, *Eur. J. Inorg. Chem.*, 2005, 4590.
11 B. K. Najafabadi and J. F. Corrigan, *Chem. Commun.*, 2014, **51**, 665.
12 (*a*) D. Fenske and F. Simon, *Angew. Chem., Int. Ed. Engl.*, 1997, **36**, 230; (*b*) X. He, H.-X. Liu and L. Zhao, *Chem. Commun.*, 2016, **52**, 5682; (*c*) X.-J. Wang, T. Langetepe, C. Persau, B.-S. Kang, G. M. Sheldrick and D. Fenske, *Angew. Chem., Int. Ed.*, 2002, **41**, 3818; (*d*) D. Fenske, C. Persau, S. Dehnen and C. E. Anson, *Angew. Chem., Int. Ed.*, 2004, **43**, 305; (*e*) M. Ueda, Z. L. Goo, K. Minami, N. Yoshinari and T. Konno, *Angew. Chem., Int. Ed.*, 2019, **58**, 14673; (*f*) Z.-A. Nan, Y. Wang, Z.-X. Chen, S.-F. Yuan, Z.-Q. Tian and Q.-M. Wang, *Chem. Commun.*, 2018, **1**, 1; (*g*) J.-W. Liu, H.-F. Su, Z. Wang, Y.-A. Li, Q.-Q. Zhao, X.-P. Wang, C.-H. Tung, D. Sun and L.-S. Zheng, *Chem. Commun.*, 2018, **54**, 4461; (*h*) L. G. AbdulHalim, M. S. Bootharaju, Q. Tang, S. Del Gobbo, R. G. AbdulHalim, M. Eddaoudi, D.-E. Jiang and O. M. Bakr, *J. Am. Chem. Soc.*, 2015, **137**, 11970; (*i*) S.-F. Yuan, Z.-J. Guan, W.-D. Liu and Q.-M. Wang, *Nat. Commun.*, 2019, **10**, 1; (*j*) C. Sun, B. K. Teo, C. Deng, J. Lin, G.-G. Luo, C.-H. Tung and D. Sun, *Coord. Chem. Rev.*, 2021, **427**, 213576; (*k*) M. S. Bootharaju, R. Dey, L. E. Gevers, M. N. Hedhili, J.-M. Basset and O. M. Bakr, *J. Am. Chem. Soc.*, 2016, **138**, 13770.
13 M. Jash, A. C. Reber, A. Ghosh, D. Sarkar, M. Bodiuzzaman, P. Basuri, A. Baksi, S. N. Khanna and T. Pradeep, *Nanoscale*, 2018, **10**, 15714.
14 A. Kulkarni, S. Arumugam, M. Francis, P. G. Reddy, E. Nag, S. M. N. V. T. Gorantla, K. C. Mondal and S. Roy, *Chem. – Eur. J.*, 2021, **27**, 200.

